Three-wave interactions among surface gravity waves in a cylindrical container

Guillaume Michel[*]

Laboratoire de Physique Statistique, École Normale Supérieure, PSL Research University, Université Paris Diderot Sorbonne Paris-Cité, Sorbonne Universités UPMC, Univ. Paris 06 and CNRS, 24 Rue Lhomond, 75005 Paris, France

The motion of a container filled with fluid perturbs the free surface and may result in spilling. In practice, most of the energy is localized in the modes of lowest frequencies (the gravest modes), and sloshing can be predicted once the dynamics of these modes is known. In this Rapid Communication, we investigate the nonlinear interactions between such grave modes in a cylindrical container. We first show that energy can be transferred from modes to modes with three-wave interactions: we derive the resonance conditions and characterize the early stage of this interaction. This result strongly contrasts with resonant interactions between surface gravity waves in extended domains such as the ocean, which involve at least four waves and are thus less efficient. An experiment is then performed to provide evidence of these nonlinear interactions.

I. INTRODUCTION

Although the study of sloshing is almost two centuries old [1], it is still extremely challenging to predict the surface deformation of a container undergoing back-and-forth oscillations. The main source of difficulties is nonlinearities, which must be taken into account starting from very small amplitudes: The experiments of Cocciaro *et al.* [2,3] have proved that the first nonlinearity to occur corrects the dissipation, and it has been recently demonstrated that, in perfect wetting, this effect becomes sizable when the sloshing amplitude compares to the thickness of the boundary layers (a fraction of millimetre in everyday life containers) [4]. This explains why, whereas natural frequencies are experimentally found in good agreement with linear sloshing theory [2,3,5–7], damping rates involve larger discrepancies [2,5–7].

As the forcing amplitude is further increased, other nonlinear phenomena arise. The natural frequencies evolve with the oscillation amplitude [8,9], and spatial and temporal harmonics appear, referred to as *bound waves* in oceanography and first studied by Stokes for plane waves [10]. The dynamics of the different modes get coupled by nonlinearities: for a cylindrical container, back-and-forth displacement at the gravest eigenfrequency may, for instance, result in a pattern rotating with a periodic or a chaotic dynamics [11,12]. Energy can also be transferred between modes of different eigenfrequencies by resonant interactions. Such energy transfers have been mainly studied in the context of oceanography, i.e., for surface gravity waves in a fluid of infinite depth and without lateral boundaries. In that case, resonant interactions involve at least four waves [13], although three-wave interactions have been recently reported in the presence of a turbulent wave background [14,15]. The associated growth rate and phase locking have been first computed by

---

[*]guillaume.michel@ens.fr

Longuet-Higgins [16] and accurately describe experimental results for a large range of parameters (see Ref. [17] and references therein).

In this Rapid Communication, we investigate how these resonant energy transfers are affected by the presence of solid boundaries. We first consider two mother waves in a resonant configuration and compute the characteristics of the daughter wave for the early stage of the interaction: three-wave resonant interactions are demonstrated to be allowed in a cylindrical geometry. We explicitly compute the growth rate as a function of the different parameters. Then, we report on an experiment able to isolate a single three-wave resonant interaction in the absence of a wave-turbulent background. The characteristics of the daughter wave are found in agreement with the theoretical predictions.

II. CHARACTERISTICS OF THE RESONANT INTERACTIONS

Consider a cylindrical container of radius R partially filled with a fluid of density ρ and of surface tension σ up to a height h. This height is thereafter assumed to be infinite, and surface tension is disregarded. In the linear potential theory of surface waves, the surface elevation $\eta(r, \theta, t)$ can then be decomposed into a sum of modes progressing clockwise or counterclockwise of the form [18]

$$A_{n,m} J_m(k_{n,m} r) \cos(\omega_{n,m} t - m\theta), \tag{1}$$

where $A_{n,m}$ is the amplitude of the mode, J_m is the Bessel function of order m (m is an integer that can be negative), $k_{n,m}$ is the wave number and is such that $k_{n,m} R$ is the nth root of J'_m, and $\omega_{n,m} = \sqrt{g k_{n,m}}$ is the angular frequency. In the linear and inviscid theory, the amplitudes $A_{n,m}$ are constant. However, if nonlinearities are taken into account, these coefficients become coupled and time-dependent, which may result in resonant energy transfers. For plane waves, these resonant interactions have been characterized either by an expansion of the continuity equation and boundary conditions at the free surface [16,19] or through a Hamiltonian formulation of the problem [20,21]. Let A and B denote two waves, thereafter called mother waves, assumed to be of constant amplitudes and of surface elevations,

$$\eta_i(r, \theta, t) = \frac{\epsilon_i}{k_i} J_{m_i}(k_i r) \cos(\omega_i t - m_i \theta), \tag{2}$$

where $i = \{A, B\}$ and ϵ_i is the steepness, i.e., a characteristic slope of the interface. The following result is derived in the Appendix: three-wave resonant interactions occur if $J'_{m_C}(\omega_C^2 R/g) = 0$, with $\omega_C = \omega_A \pm \omega_B$ and $m_C = m_A \pm m_B$ (the signs have to be the same in these two equations), i.e., if a free wave of angular frequency ω_C and index m_C exists. In that case, this daughter wave grows according to

$$k_C \eta_C(r, \theta, t) = -\kappa \frac{\omega_C^3}{4\omega_A \omega_B} \epsilon_A \epsilon_B t J_{m_C}(k_C r) \sin(\omega_C t - m_C \theta), \tag{3}$$

where $k_C = \omega_C^2/g$ is the wave number and κ is a dimensionless constant reported in Eq. (A5).

The difference between resonant interactions in a cylindrical container and in the ocean, which respectively involve at least three and four waves, can be traced back to conservation laws. Indeed, both interactions are associated with conserved quantities, as in particular the energy E, the linear pseudomomentum $\mathbf{P}$ and the angular pseudomomentum along the vertical axis L_z. For a surface wave of the form Eq. (2) of small steepness in a cylinder, the linear pseudomomentum vanishes, whereas the angular pseudomomentum is given by $L_z = mE/\omega$: the resonance conditions $\omega_C = \omega_A \pm \omega_B$ and $m_C = m_A \pm m_B$ therefore, respectively, correspond to the conservation of energy and of angular pseudomomentum. In contrast, plane progressive waves possess no angular pseudomomentum, but possess a linear pseudomomentum $\mathbf{P} = \mathbf{k}E/\omega$, and the resonant conditions become $\omega_C = \omega_A \pm \omega_B$ and $\mathbf{k}_C = \mathbf{k}_A \pm \mathbf{k}_B$. Both these resonant conditions are supplemented with the dispersion relation for the wave C, i.e., require the daughter wave to be a free wave: $\omega_C^2 = g k_C$, with either $k_C = \xi_{m_C, n_C}/R$ or $k_C = |\mathbf{k}_C|$. The main effect of solid boundaries is that, whereas this

additional constraint for the daughter wave can never be fulfilled in the case of plane waves [16], it may hold for waves in a cylindrical container.

This has strong consequences regarding the efficiency of energy transfers through nonlinear resonant interactions. For three-wave interactions, the steepness of the daughter wave is reported in Eq. (3) and scales as $\epsilon_C \sim \epsilon_A \epsilon_B \omega_C t$. A characteristic timescale for this nonlinear interaction, T_{3w}, can be obtained by assuming $\epsilon_A = \epsilon_B \equiv \epsilon$ and defining T_{3w} as the solution of $\epsilon_C(T_{3w}) = \epsilon$. We obtain $T_{3w} \sim 1/(\epsilon \omega_C)$. Conversely, if three-wave resonant interactions are forbidden, the analysis has to be pursued at the next order, in which four-wave resonant interactions are found to occur for plane progressive surface gravity waves. The steepness of the daughter wave ϵ_D then scales as [16] $\epsilon_D \sim \epsilon_A \epsilon_B \epsilon_C \omega_D t$, and, the timescale of this interaction is $T_{4w} \sim 1/(\epsilon^2 \omega_D)$. In the limit of weak nonlinearities, the steepnesses remain small and therefore $T_{4w} \gg T_{3w}$. This confirms that the presence of solid boundaries enhances nonlinear energy transfers.

III. EXPERIMENTAL STUDY

To demonstrate the efficiency of these nonlinear energy exchanges, an experiment is carried out to isolate and characterize a single three-wave resonant interaction. The main challenge is that such exchanges of energy are, most of the time, degenerate: If an interaction associated with the resonance condition,

$$\omega_C = \omega_A \pm \omega_B, \quad m_C = m_A \pm m_B, \tag{4}$$

is observed, then, since the angular frequency does not depend on the sign of m, i.e., upon the fact that the wave is rotating clockwise or counterclockwise, the following resonance condition is also verified:

$$\omega_C = \omega_A \pm \omega_B, \quad (-m_C) = (-m_A) \pm (-m_B). \tag{5}$$

This can be seen as a consequence of the symmetry of the system with respect to any plane including the vertical axis. The only situation in which such an interaction would not be degenerate is if all the waves involved are axisymmetric, that is if $m_A = m_B = m_C = 0$. Such waves are experimentally difficult to generate, and require a parametric forcing as for instance a vertical oscillation of the container (leading to the so-called Faraday instability), whereas back-and-forth oscillations of the device would force the modes $m = \pm 1$. We present below an experimental setup able to isolate a single three-wave resonant interaction with non axisymmetric waves, and we focus on the resonance of the mother waves ($m_A = 1, n_A = 1$) and ($m_B = -1, n_B = 2$) with the daughter wave ($m_C = 0$, $n_C = 3$).

The setup consists in a cylinder of diameter $2R = 18.9$ cm filled with water up to a height $h \simeq 3$ cm such that $\pi R^2 h = 950$ ml. This finite depth induces a small correction to the angular frequency of the mode A [$\tanh(k_A h) \simeq 0.6$] necessary to verify both resonance conditions Eq. (4), the frequency mismatch $\omega_C - (\omega_A + \omega_B)$ being for the present value of R too large to observe this resonance in the infinite depth limit. A motor Parvex RS420 rotates this cylinder around its vertical axis (Δ) with a constant angular frequency Ω: this rotation breaks the symmetry between counterpropagating waves and, as we shall see, enables us to isolate a single resonant triad. Another shaker LDS 555 drives an oscillation of this cylinder along an axis (Δ_v) perpendicular to (Δ), which generates surface waves. Finally, two homemade capacitive height sensors record the surface elevation 2 cm away from the vertical axis, at angles $\theta = 0$ and $\theta = \pi/2$. These signals $\eta_1(t)$ and $\eta_2(t)$ are either processed by a spectrum analyser HP 35670A or recorded with a NI-USB 4431 acquisition card. This entire experimental setup is sketched in Fig. 1.

The effect of the solid rotation of the cylinder on water waves is quantified by the nondimensional Froude number Fr $= \Omega \sqrt{R/g}$, the most notable features being that:

(1) The equilibrium free-surface on top of which the waves develop is no longer plane but parabolic at low Fr.

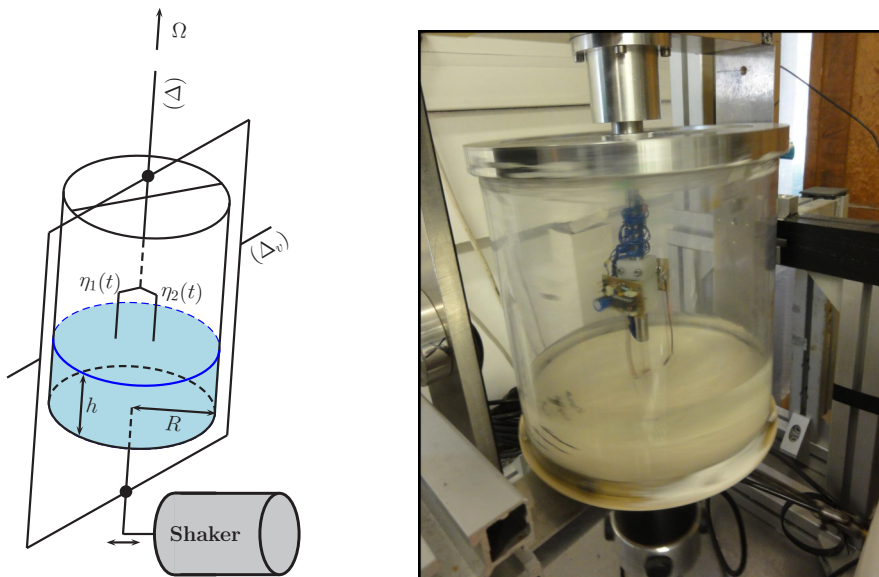(2) New waves can be observed, as inertial waves or Rossby waves.

FIG. 1. Experimental setup (sketch and photography). The notations (r, θ, z) in the text correspond to the usual cylindrical coordinate with $z = 0$ at the interface. In this experiment, $h \simeq 3\,\mathrm{cm}$ and $R \simeq 9\,\mathrm{cm}$, while a typical value of Ω is $2\pi \times 250\,\mathrm{mHz}$.

(3) The velocity fields of surface waves evolve because of the Coriolis acceleration and of the form of the free surface. The boundary layers turn to Eckman layers and the velocity fields tend to become independent on the vertical z coordinate.

In the present study, rotation is only used to disentangle counter-propagating waves, for which small Froude numbers are sufficient. In this limit $\mathrm{Fr} \ll 1$, the effects of the solid rotation on the eigenmodes reduce to a splitting of the degenerate eigenfrequencies. This has first been computed by Thomson and Rayleigh for shallow-water surface gravity waves [22,23] and has then been generalized by Miles to arbitrary depths [24]: the natural angular frequencies in the presence of rotation are given by

$$\omega_{m,n}(\Omega) = \omega_{m,n}(0) + \frac{m\Omega}{\xi_{m,n}^2 - m^2}\left[1 + \frac{2\xi_{m,n}h}{R\sinh\left(\frac{2\xi_{m,n}h}{R}\right)}\right] + O[\omega_{m,n}(0)\mathrm{Fr}^2],$$

$$\omega_{m,n}(0)^2 = \frac{g\xi_{m,n}}{R}\tanh\left(\frac{\xi_{m,n}h}{R}\right), \tag{6}$$

where $\omega_{m,n}(0)$ is the natural angular frequency in the absence of rotation. This splitting is similar to the one of acoustic modes in rotating stars (used in helioseismology, see, e.g., Ref. [25]) and to the Zeeman effect in optics. The effect of surface tension is discussed in Ref. [26] and large Froude numbers in Ref. [27]. According to Eq. (6), the resonance condition $\omega_A + \omega_B = \omega_C$ for the parameters $\{m_i, n_i\}$ mentioned above occurs for a rotation frequency of $242\,\mathrm{mHz}$, associated to a Froude number of 0.25.

The first experiment we conduct consists in driving the shaker with a noise of bandwidth [0, 4 Hz], for several rotation rates Ω. Power spectra of the surface elevation are reported in Fig. 2 left, and reveal three major contributions in the forcing range: two peaks around 1.8 Hz evidencing the splitting of the gravest eigenmode ($m = \pm1$, $n = 1$), and a third one around 3.8 Hz corresponding to the modes ($m = \pm1$, $n = 2$). A signal of angular frequency Ω and a harmonic at 2Ω are also measured (see Fig. 2) as a result of mechanical imperfections during the rotation.
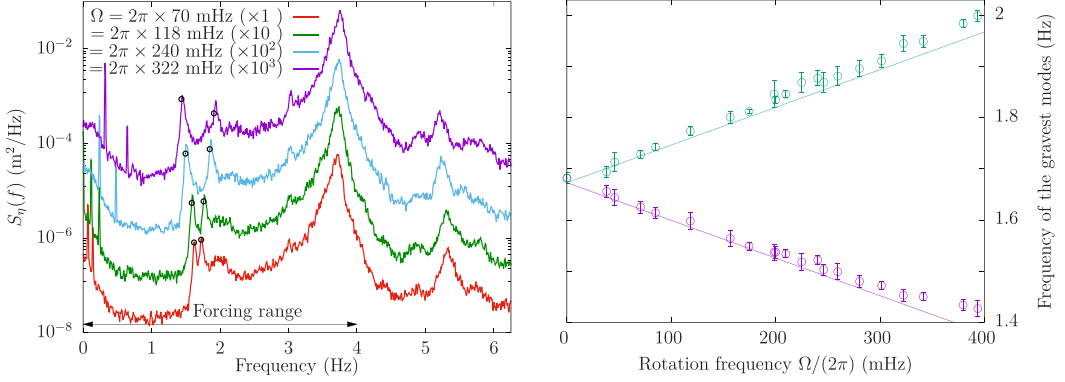
FIG. 2. Left: Surface elevation power spectrum. The black circles are the theoretical resonance frequencies (see right graph). Right: Experimental natural frequencies of the gravest modes, compared to the theoretical prediction of Eq. (6) derived in the limit of small Froude numbers

Finally, a component of frequency close to 5.3 Hz is observed and cannot be ascribed to the forcing: it corresponds to the daughter wave $m_C = 0$ and $n_C = 3$, as shall be shown from three of its characteristics.

From these spectra, the theoretical result Eq. (6) of Miles [24] is found to accurately describe our experiment without any fitting parameter [see Fig. 2 (right)]. The splitting of the other modes of frequency close to 3.8 Hz is proportional to $1/(\xi_{\pm 1,2}^2 - 1^2) \simeq 0.04$ [see Eq. (6)] and cannot be resolved with this setup. From the spectrum reported in Fig. 2 (left), it is visible that the frequency of the peak out of the forcing range slightly decreases as the rotation rate increases: We checked that its angular frequency matches $\omega_{+1,1} + \omega_{-1,2}$, i.e., is related to the gravest peak. This first result confirms that the resonance condition in terms of frequencies holds, i.e., that $\omega_C = \omega_A + \omega_B$ in Eq. (4).

In a second experiment, the rotation frequency is fixed at 240 mHz, with the same forcing as above. The simultaneous acquisition of the surface elevation at two different positions through the signals $\eta_1(t)$ and $\eta_2(t)$ is now used. More precisely, the phase of the cross-spectral density is computed, defined as

$$\varphi_{\eta_1,\eta_2}(f) = \text{Angle}\left[\iint_{-\infty}^{\infty} \eta_1(t)\eta_2(t+\tau)e^{2i\pi f\tau}dt d\tau\right]. \qquad (7)$$

When the signals η_1 and η_2 are correlated for a given frequency f, $\varphi_{\eta_1,\eta_2}(f)$ converges toward the phase shift between them. For instance, taking $\eta_1 \propto \cos(2\pi f t)$ and $\eta_2 \propto \cos(2\pi f t - \varphi_0)$ leads to $\varphi_{\eta_1,\eta_2}(f) = \varphi_0$. In the present experiment, the two signals are correlated when the surface elevation corresponds to an eigenmode of the form $\eta \propto \cos(2\pi f t - m\theta)$. Since $\eta_1(t) = \eta(r_0, \theta = 0, t)$ and $\eta_2(t) = \eta(r_0, \theta = \pi/2, t)$ with $r_0 = 2$ cm, we obtain $\varphi_{\eta_1,\eta_2}(f) = m\pi/2$. Thus, the measurement of φ gives access to the angular index m. The results obtained from the experiment are reported in Fig. 3 (left). Consistently with the previous results, the couple of peaks around 1.7 Hz are found to be associated to $m = \pm 1$, the gravest one being $m_A = 1$. Moreover, the wave field at $\omega_B \simeq 2\pi \times 3.7$ Hz is dominated by the component $m_B = -1$. The main result is that the daughter wave is indeed a mode of angular index $m_C = 0$. This also confirms that such mode cannot be directly excited through back and forced oscillation of the cylinder, and therefore results from nonlinear interactions. This verifies the second resonant condition $m_C = m_A + m_B$ in Eq. (4).

In a third experiment, the rotation frequency is fixed, as before, at 240 mHz, and the gain of the amplifier driving the shaker is varied. Since the spectrum consists in well-defined peaks, we can evaluate a quantity E_i proportional to the energy of each mode by integrating the power-spectra
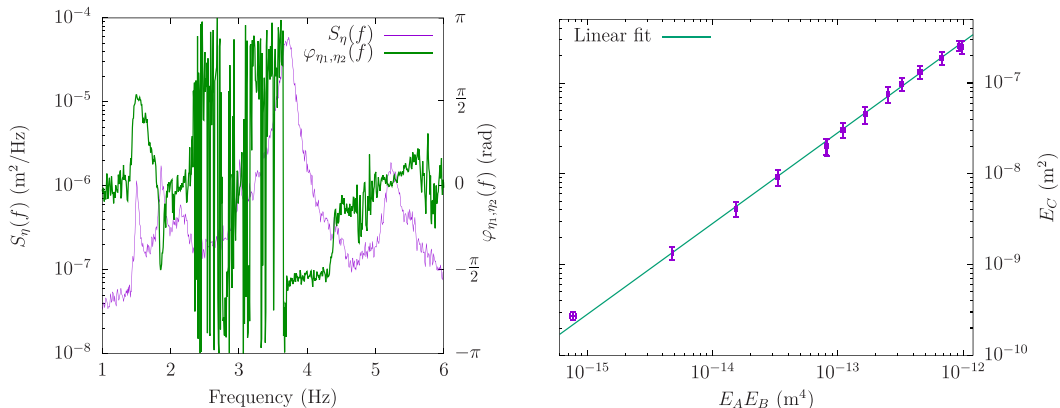
FIG. 3. Left: surface elevation spectra and phase of the cross-spectral density for $\Omega = 2\pi \times 0.240$ mHz. Right: Evolution of a measure of the energy of the daughter wave with the ones of the mother waves.

over a fixed and constant frequency window,

$$E_i = \int_{f_i - \Delta f}^{f_i + \Delta f} S_\eta(f) df. \tag{8}$$

Note that although these quantities E_i slightly depend upon the choice of Δf, their relative variations considered here do not. In Fig. 3 (right), we show that the relation $E_C \propto E_A \times E_B$ is verified over four decades. This is consistent with the quadratic energy flux from the mother waves to the daughter one of Eq. (3).

Therefore, the experiments reported here confirm the characteristics of these three-wave interactions between gravity waves in a cylinder: both resonance conditions are observed ($\omega_C = \omega_A + \omega_B$ and $m_C = m_A + m_B$), along with a quadratic relation of the form $\eta_C \propto \eta_A \times \eta_B$. Note that the theoretical work performed in the Appendix does not model exactly these experiments, because the depth is not infinite, the surface tension is nonzero and rotation affects the dynamics. However these corrections remain small. Indeed, the finite-height only slightly affects the gravest mode: the non-dimensional number $\tanh(kh)$ introduced in Eq. (6) quantifies this effect and is 0.6 for the wave A, and 0.98 or more for the modes B and C. The largest frequency considered here, 5.3 Hz, also is small compared to the one at which the transition from gravity waves to capillary waves occurs ($f_{\text{g.c.}} = 1/(2\pi)(4\rho g^3/\sigma)^{1/4} = 13$ Hz in water, where $g = 9.81$ m s^{-2} is the acceleration of gravity, $\sigma = 75$ mN m^{-1} is the surface tension and $\rho = 10^3$ kg m^{-3} is the density of water): since no high-frequency parasitic capillary wave is observed, as evident from the absence of high-frequency peak in the surface elevation power spectra, surface tension can be consistently neglected. Regarding the solid rotation, the Froude number at resonance Fr = 0.25 remains small compared to unity. Note that dissipation would have to be taken into account to describe these steady states, in particular for the last set of experiments. This is usually done by adding a linear damping term in the evolution equations of each mode (see, e.g., Refs. [11,12]). However, such linear damping coefficients have to be measured experimentally and are very sensitive to the pollution of the free surface, especially for water. In practice, nonlinear damping has to be considered when experiments are performed in a small container as a result of the walls. In addition to the nonlinear energy exchanges, this makes the quantitative study of these steady states very challenging.

IV. CONCLUSION

In this Rapid Communication, resonant interaction between gravity waves in a circular container are characterized theoretically and experimentally. Unlike plane waves in the ocean, which undergo four-wave or higher interactions, this geometry allows for three-wave resonant interactions. This

effect traces back to the resonance conditions, in which the conservation of linear pseudomomentum is replaced by the conservation of angular pseudomomentum. The resonance conditions and the linear growth rate are derived. An experiment able to isolate a single resonant triad, achieved by adding a small rotation to the container, is then performed to characterize the resonance. Both the resonant condition in term of angular frequency ω and of angular index m are observed, along with the quadratic nature of these energy exchanges.

Such resonant interactions are of crucial importance for, at least, two separate outlooks. The first one deals with sloshing control, that aims at a reduction of the energy of the gravest eigenmode (denoted as wave A here). In this perspective, deliberately forcing another eigenmode (wave B) would result in a transfer of energy toward wave C and therefore act as an efficient damping mechanism for the mother waves. The study of such energy exchanges in a steady state, with dissipation and presumably out of the weakly nonlinear limit, would be required to fully discuss this point. A second motivating follow-up concerns wave turbulence, which predicts the statistical properties of a chaotic state in which many plane waves of small amplitudes, different frequencies, and different directions interact with one another [28]. The results of this theory strongly depend on the minimal number of waves involved in a resonant interaction, and the statistics of the gravest modes in the case of a cylindrical vessel, for instance, measured experimentally in Refs. [29,30], are still an open question that would require to take into account the three-wave interactions reported in the present study. This remark is not restricted to gravity surface waves. The minimal number of planes waves involved in a resonant interaction can be determined from the dispersion relation (see, e.g., Ref. [28]): for instance, capillary surface waves, hydroelastic waves and internal waves in stratified and/or rotating fluids can undergo resonant three-wave interactions, whereas elastic waves in thin plates and deep-water gravity waves cannot. Therefore, depending on the geometry of the experimental apparatus, the gravest modes in all of these examples may not be accurately described by plane waves and this minimal number of waves may vary, as shown here for gravity surface waves in a cylindrical vessel.

ACKNOWLEDGMENTS

APPENDIX

We consider a cylinder of radius R filled with an infinite depth of water: the usual (r, θ, z) cylindrical coordinate system is used, $z = 0$ corresponding to the interface between water and air. In the potential theory, the surface elevation η_i [Eq. (2)] of the mother waves corresponds to a velocity field

$$\vec{u}_i = -\vec{\nabla}\big[\Psi_i J_{m_i}(k_i r)e^{k_i z}\sin(\omega_i t - m_i \theta)\big] = -\vec{\nabla}\phi_i, \tag{A1}$$

with $\epsilon_i = \Psi_i k_i^2 / \omega_i$ [18]. As derived by Longuet-Higgins [16], the leading order correction describing the nonlinear coupling between these two waves $i = \{A, B\}$, $\vec{u}_C = -\vec{\nabla}\phi_C$, is the solution of

$$\partial_{tt}\phi_C + g\partial_z\phi_C \underset{z=0}{=} 2\partial_t(\vec{u}_A \cdot \vec{u}_B), \quad \partial_r\phi_C \underset{r=R}{=} 0, \quad \triangle\phi_C = 0. \tag{A2}$$

Using recurrence relations of Bessel functions, we obtain

$$\begin{aligned}(\vec{u}_A \cdot \vec{u}_B) \underset{z=0}{=} \frac{\psi_A \psi_B k_A k_B}{4}\big[&\big(2J_{m_A}J_{m_B} + J_{m_A+1}J_{m_B+1} + J_{m_A-1}J_{m_B-1}\big)\cos(\varphi_A - \varphi_B) \\ &+ \big(-2J_{m_A}J_{m_B} + J_{m_A+1}J_{m_B-1} + J_{m_A-1}J_{m_B+1}\big)\cos(\varphi_A + \varphi_B)\big],\end{aligned} \tag{A3}$$

where $\varphi_i = \omega_i t - m_i \theta$ is the total phase of the wave i. The remainder of the analysis consists in determining whether this term resonantly forces a free wave in Eq. (A2). To do so, Eq. (A3) is expanded in Dini series,

$$(\vec{u}_A \cdot \vec{u}_B) \underset{z=0}{=} \sum_n \alpha_n J_{m_A - m_B}\left(\xi_{n,m_A - m_B}\frac{r}{R}\right)\cos(\varphi_A - \varphi_B)$$

$$+ \sum_n \beta_n J_{m_A + m_B}\left(\xi_{n,m_A + m_B}\frac{r}{R}\right)\cos(\varphi_A + \varphi_B), \tag{A4}$$

where $\xi_{n,m}$ is the nth root of J'_m, and the coefficients $\{\alpha_n, \beta_n\}$ result from orthogonality relations. In particular,

$$\beta_n = \frac{\Psi_A \Psi_B k_A k_B}{4}\kappa, \quad \kappa = \frac{\int_0^1 x J_{m_C}(\xi_{n,m_C}x)\left[-2J_{m_A}J_{m_B} + J_{m_A+1}J_{m_B-1} + J_{m_A-1}J_{m_B+1}\right]dx}{\int_0^1 x J_{m_C}^2(\xi_{n,m_C}x)dx}, \tag{A5}$$

where J_{m_i} is a shorthand for $J_{m_i}(\xi_{n_i,m_i}x)$. Since Eq. (A2) is a linear equation we consider a single term in Eq. (A4), of the form $\beta_n J_{m_C}(k_C)\cos[\omega_C t - m_C\theta]$, with $m_C = m_A + m_B$, $\omega_C = \omega_A + \omega_B$ and $k_C = \xi_{n,m_A+m_B}/R$. The velocity potential forced by this term is a solution of Eq. (A2) with $2\partial_t(\vec{u}_A \cdot \vec{u}_B) = -2\omega_C\beta_n J_{m_C}(k_C r)\sin[\omega_C t - m_C\theta]$. This system has two very different sets of solutions: a surface wave of constant amplitude that does not follow the linear dispersion relation (a "bound wave") if $\omega_C^2 \neq gk_C$, and a linearly growing "free wave" if $\omega_C^2 = gk_C$, of the form

$$\phi_C = \beta_n t J_{m_C}(k_C r)\cos[\omega_C t - m_C\theta]e^{k_C z} \Rightarrow \eta_C = -\frac{\beta_n k_C t}{\omega_C}J_{m_C}(k_C r)\sin[\omega_C t - m_C\theta]. \tag{A6}$$

Equations (A5) and (A6) lead to the result Eq. (3). Finally, note that Eq. (3) evidences a phase locking between the waves: with both mother waves of the form $\cos(\omega_i t - m_i\theta)$, the resulting daughter wave is proportional to $\sin(\omega_i t - m_i\theta)$.

---

[1] S. D. Poisson, Hydrodynamique. Mémoire sur les petites oscillations de l'eau contenue dans un cylindre, Annales de mathématiques pures et appliquées **19**, 225 (1828), http://www.numdam.org/item/AMPA_1828-1829__19__225_0/.

[2] B. Cocciaro, S. Faetti, and M. Nobili, Capillarity effects on surface gravity waves in a cylindrical container: Wetting boundary conditions, J. Fluid Mech. **231**, 325 (1991).

[3] B. Cocciaro, S. Faetti, and C. Festa, Experimental investigation of capillarity effects on surface gravity waves: Nonwetting boundary conditions, J. Fluid Mech. **246**, 43 (1993).

[4] G. Michel, F. Pétrélis, and Stéphan Fauve, Observation of nonlinear sloshing induced by wetting dynamics, Phys. Rev. Fluids **2**, 022801 (2017).

[5] K. M. Case and W. C. Parkinson, Damping of surface waves in an incompressible liquid, J. Fluid Mech. **2**, 172 (1956).

[6] D. M. Henderson and J. W. Miles, Surface-wave damping in a circular cylinder with a fixed contact line, J. Fluid Mech. **275**, 285 (1994).

[7] D. R. Howell, B. Buhrow, T. Heath, C. McKenna, W. Hwang, and M. F. Schatz, Measurements of surface-wave damping in a container, Phys. Fluids **12**, 322 (2000).

[8] L. R. Mach, Periodic, finite-amplitude, axisymmetric gravity waves, J. Geophys. Res. **67**, 829 (1962).

[9] D. Fultz and T. S. Murty, Experiments on the frequency of finite-amplitude axisymmetric gravity waves in a circular container, J. Geophys. Res. **68**, 1457 (1963).

[10] G. G. Stokes, On the theory of oscillatory waves, Camb. Trans **8**, 441 (1847); see also G. B. Whitham, *Linear and Nonlinear Waves* (John Wiley & Sons, New York, 1974).

[11] J. W. Miles, Internally resonant surface waves in a circular cylinder, J. Fluid Mech. **149**, 1 (1984).

[12] J. W. Miles, Resonantly forced surface waves in a circular cylinder, J. Fluid Mech. **149**, 15 (1984).

[13] O. M. Phillips, On the dynamics of unsteady gravity waves of finite amplitude. Part 1. The elementary interactions, J. Fluid Mech. **9**, 193 (1960).

[14] Q. Aubourg and N. Mordant, Nonlocal Resonances in Weak Turbulence of Gravity-Capillary Waves, Phys. Rev. Lett. **114**, 144501 (2015).

[15] Q. Aubourg and N. Mordant, Investigation of resonances in gravity-capillary wave turbulence, Phys. Rev. Fluid **1**, 023701 (2016).

[16] M. S. Longuet-Higgins, Resonant interactions between two trains of gravity waves, J. Fluid Mech. **12**, 321 (1962).

[17] F. Bonnefoy, F. Haudin, G. Michel, B. Semin, T. Humbert, S. Aumaître, M. Merhanu, and E. Falcon, Observation of resonant interactions among surface gravity waves, J. Fluid Mech. **805**, R3 (2016).

[18] R. A. Ibrahim, *Liquid Sloshing Dynamics* (Cambridge University Press, New York, 2005).

[19] K. Hasselmann, On the non-linear energy transfer in a gravity-wave spectrum. Part 1. General theory, J. Fluid Mech. **12**, 481 (1962).

[20] V. E. Zakharov, Stability of periodic waves of finite amplitude on a surface of a deep fluid, J. Appl. Mech. Tech. Phys. **9**, 190 (1968).

[21] P. A. E. M. Janssen, On some consequences of the canonical transformation in the Hamiltonian theory of water waves, J. Fluid Mech. **637**, 1 (2009).

[22] W. Thomson, On gravitational oscillations of rotating water, Proc. R. Soc. Edinburgh **10**, 92 (1880).

[23] L. Rayleigh, On the free vibrations of systems affected with small rotatory terms, Phil. Mag. S. 6. **5**, 10 (1903).

[24] J. W. Miles, Free-surface oscillations in a slowly rotating liquid, J. Fluid Mech. **18**, 187 (1964).

[25] T. G. Cowling and R. A. Newing, The oscillations of a rotating star, Astrophys. J. **109**, 149 (1949).

[26] H. F. Bauer and W. Eidel, Axisymmetric oscillations in a slowly rotating cylindrical container filled with viscous liquid, Forsch. Ingwes. **63**, 215 (1997).

[27] J. Mougel, D. Fabre, and L. Lacaze, Waves in Newton's bucket, J. Fluid Mech. **783**, 211 (2015).

[28] S. Nazarenko, *Wave Turbulence* (Springer-Verlag, Berlin, Heidelberg, 2001); V. E. Zakharov, V. S. Lvov, and G. Falkovich, *Kolmogorov Spectra of Turbulence 1: Wave Turbulence*, Series in Nonlinear Dynamics (Springer, Berlin, 1992).

[29] L. Deike, M. Berhanu, and E. Falcon, Decay of capillary wave turbulence, Phys. Rev. E **85**, 066311 (2012).

[30] L. Deike, M. Berhanu, and E. Falcon, Energy flux measurement from the dissipated energy in capillary wave turbulence, Phys. Rev. E **89**, 023003 (2014).